Crystallization in Nonaqueous Media of Co- and Mn-Substituted Microporous Aluminophosphates Investigated by *in Situ* Synchrotron X-ray Powder Diffraction

P. Norby* and A. Nørlund Christensen

Department of Inorganic Chemistry, Aarhus University, DK-8000 Aarhus C, Denmark

J. C. Hanson

Chemistry Department, Brookhaven National Laboratory, Upton, New York 11973

Received June 30, 1998

In situ synchrotron X-ray powder diffraction was used to investigate the crystallization of microporous transition metal-substituted aluminophosphates from nonaqueous media. The gels contained ethylene glycol and triethylamine as the template and were heated in quartz glass capillaries at temperatures up to 200 °C. The following crystalline products were formed: MnAPO-5, [AFI], CoAPO-5, [AFI], and $AlPO_4$-5, [AFI]. Three nonaqueous systems were investigated *in situ*, where the crystallization of MAPO-5-type materials were followed. Solvothermal crystallization of MnAPO-5 and CoAPO-5 was studied, and the effect of adding HF as a mineralizing agent was investigated. Time-resolved powder diffraction data were collected using a translating imaging plate (TIP) camera, and crystallization curves were extracted using integrated diffraction peaks. Kinetic analysis of the crystallization curves was performed using an Avrami-type expression, $\alpha(t) = \exp(-(kt)^n)$. Apparent activation energies were determined from Arrhenius plots: MnAPO-5, 94 kJ/mol; MnAPO-5(HF), 68 kJ/mol; CoAPO-5, 61 kJ/mol. Crystallization of CoAPO-5 is faster than for MnAPO-5, and the values for *n* obtained by fitting with the Avrami-type expression were significantly lower for CoAPO-5 than for MnAPO-5.

Introduction

Microporous aluminophosphates ($AlPO_4$-*n*)[1] and metal-substituted aluminophosphates (MAPOs)[2] are prepared by aqueous hydrothermal synthesis from amorphous aluminophosphate gels containing organic amines as structure-directing templates. This type of synthesis under pressure at temperatures above the ambient boiling point of the solvent in the reaction mixture can also be made in nonaqueous media. This will in the following be termed "solvothermal synthesis". Synthesis of aluminophosphate-based molecular sieves from nonaqueous systems were reported by Huo and Xu.[3] They obtained $AlPO_4$-5, $AlPO_4$-11, and $AlPO_4$-21 using the solvent−template combinations ethylene glycol−triethylamine, ethylene glycol−dipropylamine, and ethylene glycol−ethylamine, respectively. A number of papers have been published on nonaqueous synthesis of microporous or layered phosphates, mainly by using ethylene glycol as the solvent, but also the use of pyridine, poly(ethylene glycol), and other alcohols have been reported.[3−12] Aluminophosphate molecular sieves grown in nonaqueous media may have crystal dimensions in the size range 0.4−5.0 mm, when hydrofluoric acid is used as a mineralizer.[4] The use of this mineralizer can also drastically improve the crystal size in the aqueous hydrothermal synthesis of metal-substituted aluminophosphates (CrAPO-5).[13]

In situ synchrotron X-ray powder diffraction has been used to study the crystallization of microporous $AlPO_4$-*n* and of MAPOs. Detailed information has been gained including identification of crystalline precursor phases and determination of apparent activation energies for crystallization.[14−17] Such *in situ* investigations have not been reported on the nonaqueous synthesis of $AlPO_4$-*n* and of MAPOs.

The rate of formation and the size of crystals formed in hydrothermal synthesis from an aqueous gel can be related to the solubility of the particles in the gel, the rate of formation of nuclei, and the solubility of the reaction product.[18] A high nucleation rate results in many small crystals and is the case

* To whom correspondence should be addressed. Tel: +45 8942 3885. Fax: +45 8619 6199. E-mail: norby@kemi.aau.dk.

(1) Wilson, S. T.; Lok, B. M.; Flanigen, E. M. U.S. Pat. 4310440, 1982.
(2) Flanigen, E. M.; Lok, B. M.; Patton, R. L.; Wilson, S. T. *Stud. Surf. Sci. Catal.* **1986**, *28*, 103.
(3) Huo, Q.; Xu, R. *J. Chem. Soc., Chem. Commun.* **1990**, 783.
(4) Kuperman, A.; Nadimi, S.; Oliver, S.; Ozin, G. A.; Garcès, J. M.; Olken, M. M. *Nature* **1993**, *365*, 239.
(5) Xu, R.; Huo, Q.; Pang, W. *Proceedings of the 9th International Zeolite Conference*; Montreal, 1992, von Ballmos, R. et al., Eds.; Butterworth-Heinemann: London, 1993; p 271.
(6) Song, T.; Hursthouse, M. B.; Chen, J.; Xu, J.; Malik, K. M. A.; Jones, R. H.; Xu, R.; Thomas, J. M. *Adv. Mater.* **1994**, *6*, 679.
(7) Song, T.; Xu, J.; Zhao, Y.; Yue, Y.; Xu, Y.; Xu, R.; Hu, N.; Wei, G.; Jia, H. *J. Chem. Soc., Chem. Commun.* **1994**, 1171.
(8) Bu, X.; Feng, P.; Stucky, G. D. *J. Solid State Chem.* **1996**, *125*, 243.
(9) Gao, Q.; Chen, J.; Li, S.; Xu, R.; Thomas, J. M.; Light, M.; Hursthouse, M. B. *J. Solid State Chem.* **1966**, *127*, 145.
(10) Gao, Q.; Li, S.; Xu, R.; Yue, Y. *J. Mater. Chem.* **1996**, *6*, 1207.
(11) Oliver, S.; Kupermann, A.; Lough, A.; Ozin, G. A. *J. Mater. Chem.* **1997**, *7*, 807.
(12) Feng, P.; Bu, X.; Stucky, G. D. *Nature* **1997**, *388*, 735.
(13) Radaev, S. F.; Joswig, W.; Baur, W. H. *J. Mater. Chem.* **1996**, *6*, 1413.
(14) Christensen, A. N.; Norby, P.; Hanson, J. C. *Acta Chem. Scand.* **1997**, *51*, 249.
(15) Christensen, A. N.; Norby, P.; Hanson, J. C. *Microporous and Mesoporous Materials* **1998**, *20*, 349.
(16) Christensen, A. N.; Jensen, T. R.; Norby, P.; Hanson, J. C. *Chem. Mater.* **1998**, *10*, 1688.
(17) Cheetham, A. K.; Mellot, C. F. *Chem. Mater.* **1997**, *9*, 2269.
(18) Zhdanov, S. P. *Adv. Chem. Ser.* **1971**, *101*, 20.

10.1021/ic980749z CCC: $18.00
Published on Web 02/26/1999

when the solubility of the reaction product is low. The solubility in the aqueous medium at hydrothermal conditions is a priori different from the solubility in the nonaqueous medium at solvothermal conditions. It is thus of interest to investigate if *in situ* investigations of the crystallization process at solvothermal conditions can be correlated to the formation of large crystals of microporous compounds at these conditions for the synthesis.

In the present study, time-resolved *in situ* powder diffraction investigations were made to clarify and compare crystallization characteristics of Co- and Mn-substituted microporous aluminophosphates. The materials obtained were CoAPO-5 and MnAPO-5, with structure type [AFI].[19] In addition, the effect on crystallization upon adding hydrofluoric acid to the reaction mixture was studied. Kinetic analyses were performed using Avrami-type rate expressions.

Theory

Crystallization curves can be estimated from time-resolved *in situ* powder diffraction patterns by using integrated intensities of diffraction peaks. The sum of a number of integrated intensities is calculated and normalized so that the maximum intensity, after the crystallization is completed, is 1. A necessary assumption is that the intensity of the diffraction peaks from one phase is linearly dependent upon the total volume of crystalline material of that phase. When only one phase is present, the obtained crystallization curve is a direct measure of the crystal volume fraction, α.

The crystallization curves can then be fitted, using least-squares methods, with a kinetic expression, for instance, a modified Avrami expression:[20,21]

$$\alpha(t) = 1 - \exp(-(k(t - t_0))^n) \qquad (1)$$

α is the crystal volume fraction, k is a rate constant, and t_0 is the time before crystallization starts, usually interpreted as the nucleation time. When $t_0 = 0$, eq 1 can be written as

$$\alpha(t) = 1 - \exp(-(kt)^n) \qquad (2)$$

Compared to the usual Avrami equation frequently used for describing zeolite crystallization curves, the rate constant (k) has been included to the nth power.[20] Therefore, it is achieved that the unit for the rate constant becomes time^{-1} for all values of n and that a comparison between rate constants and apparent activation energies are independent of n. Figure 1 shows crystallization curves calculated using eq 2. The curves were calculated using the same k value but varying n from 1 to 10. (For $n = 1$ the expression is reduced to a regular first-order rate expression.) As can be seen from eq 2 and Figure 1, all curves intersect when $kt = 1$, i.e., $t = 1/k$. The corresponding value of α, independent of n, is $\alpha(1/k) = 1 - e^{-1} = 0.632$.

In other words, for any crystallization curve, which can be described by an Avrami equation, and for which $t_0 = 0$, the rate constant can be determined, independent of n, as the reciprocal of the time where the degree of crystallization has reached 63%, $k = 1/t_{0.63}$. When using crystallization times to estimate rate constants and apparent activation energies, $t_{0.63}$ should be used instead of the commonly used $t_{0.5}$ in order to avoid influence from variations in n.

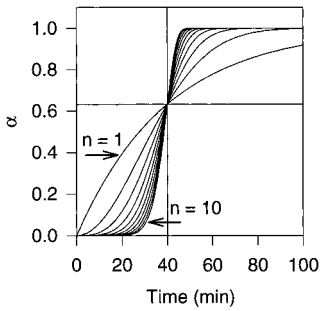

Figure 1. Calculated crystallization curves using eq 2: $\alpha(t) = 1 - \exp(-(kt)^n)$. Curves were calculated using n values from 1 to 10 with a constant value of k (0.025 min^{-1}). The curves intersect at $\alpha = 0.63 = 1 - e^{-1}$ at time $t = 40$ min $= 1/k$.

Qualitatively described, the curves in Figure 1 demonstrate that by increasing the value of n (keeping k constant), the crystallization curve becomes more flat in the beginning. The subsequent acceleration of the crystallization increases with n, and the crystallization reaches completion faster as n increases.

It must be emphasized that the Avrami equation was originally derived to describe nucleation and crystallization of metals in finite volumes.[22−24] Furthermore, the expression used most frequently to describe, e.g., zeolite crystallization, as, for instance, eq 2, is an approximation to the very early nucleation/crystallization period and is not intended to describe the full crystallization curve.[23] Last, the inclusion of a variable n value is in contrast to the original expression, where $n = 4$. The Avrami expression is therefore, in connection with zeolite crystallization, an empirical rate expression. However, many crystallization curves can be very well described using the Avrami equation, and it seems that some information regarding the nucleation and crystallization mechanisms can be related to the observed values of n.

Another approach to describing zeolite crystallization kinetics is the population balance method, which attempts to quantitatively describe zeolite nucleation and crystallization.[25] Using a reduced population balance expression, the first part of a crystallization curve is sometimes fitted using a power law:[25,26]

$$\alpha = a(t - t_0)^q \qquad (3)$$

The value of q, like the value of n in the Avrami expression, has been associated with specific crystallization mechanisms. Thus, values of q larger than 4 have been associated with "autocatalytic nucleation", where the nucleation rate increases explosively as new nucleation centers are released from the parent gel.[25]

Rate constants extracted from crystallization curves obtained at different temperatures can be plotted in an Arrhenius plot and, if the plot of ln(k) vs $1/T$ is linear, an apparent activation energy, E_A, can be found:

$$\ln(k) = -E_A/RT \qquad (4)$$

Although the k values extracted from crystallization curves strictly speaking are not true rate constants, and the derived activation energies are not true activation energies, the values

(19) Meier, W. M.; Olson, D. H. *Atlas of Zeolite Structure Types*, 3rd revised ed.; Butterworth-Heinemann: London, 1992; p 26.
(20) Sheridan, A. K.; Anwar, J. *Chem. Mater.* **1996**, *8*, 1042.
(21) Putnis, A. *Introduction to mineral sciences*; Cambridge University Press: Cambridge, 1992.
(22) Avrami, M. *J. Chem. Phys.* **1940**, *8*, 212.
(23) Thompson, R. W.; Dyer, A. *Zeolites* **1985**, *5*, 202.
(24) Thompson, R. W. *Zeolites* **1992**, *12*, 680.
(25) Katovif, A.; Subotif, B.; Smit, I.; Despotovif, L. A. *Zeolites* **1989**, *12*, 634.
(26) Sheikh, A. Y.; Jones, A. G.; Graham, P. *Zeolites* **1996**, *16*, 164.

Table 1. Compositions Listed as Molar Ratios of Gels[a]

name of gel	template TEA	MeO	Al_2O_3	P_2O_5	HF	solvent	pH of gel	reaction product crystallization expt
MnAPO	1.00	MnO 0.13	0.90	1.00		ETG 12.3	5.1	MnAPO-5, [AFI]
MnAPO−HF	1.00	MnO 0.25	0.80	1.00	0.29	ETG 14.0	5.2	MnAPO-5, [AFI]
CoAPO	1.00	CoO 0.11	0.65	1.00		ETG 14.2	4.6	CoAPO-5, [AFI]
APO	1.09		0.77	1.00		H_2O 106	5.4	$AlPO_4$-5, [AFI]

[a] The organic solvent used was ethylene glycol, ETG, and the template used was triethylamine, TEA.

extracted can be valuable for comparison between related crystallization systems.

When the Avrami expression is used to describe hydrothermal zeolite crystallization, it is of course essential to use the same definition of the rate constants, to compare derived apparent activation energies. If the rate constants have been determined using the expression $\alpha(t) = 1 - \exp(-kt^n)$, the apparent activation energies determined must be scaled by $1/n$ in order to compare them with values determined using rate constants found by eq 2.

Experimental Section

Sample Preparation. The chemicals used in the preparation of the gels were 85% H_3PO_4, 40% HF and ethylene glycol from Merck, and 98% aluminum isopropoxide, triethylamine, $Mn(CH_3COO)_2 \cdot 4H_2O$, and $Co(CH_3COO)_2 \cdot 4H_2O$ from Aldrich. A 50−100 mL charge of each gel was prepared, sufficiently large for all synthesis and diffraction experiments performed. The following procedure was applied in the preparation of the ethylene glycol-based gels: The transition metal acetate and the aluminum isopropoxide were stirred with the ethylene glycol for approximately 1 h. Then the 85% H_3PO_4 was added dropwise, the mixture was stirred for at least 15 min, the triethylamine was then added dropwise with continuous stirring, and stirring was continued for at least 30 min to obtain homogeneity. The HF was then finally added from a polyethylene pipet. The pH of the gels was measured using a pH meter, and the charges were stored at room temperature in flasks of polyethylene. The compositions of the gels are listed as molar ratios in Table 1. The gels are strictly speaking not purely nonaqueous as they contain water from the 85% H_3PO_4 and from the transition metal acetates. The APO-gel was made with water as the solvent.

Preliminary crystallization experiments were made in the laboratory at 180 °C with samples of the gels charged in Teflon containers in pressure vessels, and the crystalline reaction products so obtained were identified from their X-ray powder patterns (Table 1).

No chemical analysis of the reaction products were performed, but a general composition can be given as

$$L(n^+)_{x/n}Al_{12-x}M(II)_xP_{12}O_{48} \cdot y\text{TEA} \cdot z\text{ETG} \cdot z'H_2O$$

where $L(n^+)$ is a counterion (Mn^{2+}, Co^{2+}, or H^+) and M is Mn(II) or Co(II) substituted into the framework. The degree of substitution is usually <10%.

***In Situ* Measurements.** The *in situ* synchrotron X-ray powder diffraction investigations of the gels were made at the Huber diffractometer at beam line X7B at NSLS, Brookhaven National Laboratory. The samples were kept in 0.7 mm diameter quartz glass capillaries at an internal pressure of up to 1200 kPa. The quartz glass capillaries can withstand this internal pressure, supplied from a nitrogen gas tank, and as the volume of the sample is small, the risk in connection with the pressure experiments is minimal. The internal pressure suppresses the formation of gas bubbles in the heated part of the capillary. The capillaries were heated with a stream of hot air, and the temperature was monitored with a thermocouple placed in the stream of hot air ca. 2 mm from the capillary. The relation between the temperature in the capillaries and the monitored temperature was obtained by measurement of the unit cell parameters of a sample of microcrystalline silver prepared by thermal decomposition of silver carbonate. The powder patterns of a sample of powdered silver housed in a 0.5 mm diameter quartz glass capillary were recorded at different temperatures. The unit cell parameters of silver were then calculated using a least-squares fit, and from the thermal expansion data for silver[27] a calibration curve of temperature in the capillaries vs monitored temperature was derived. The powder patterns were recorded on a translating imaging plate (TIP) system[28] using Fuji imaging plates. The continuous powder diffraction traces on the imaging plates are very adequate for a detailed study of phase transition and of transformation of amorphous samples to crystalline products. The wavelength used was 1.1014(1) Å, calculated from a powder pattern of a LaB_6 standard[28] (NIST SRM 660a, a = 4.156 95 Å). Bragg reflections were typically recorded out to $\sin\theta/\lambda = 0.56$, and the crystalline compounds formed were identified from their X-ray powder patterns. Further details of the *in situ* methods using X-ray synchrotron powder diffraction have been reported previously.[28−30]

Crystallization curves for the isothermal formation of MnAPO-5, MnAPO-5(HF), and CoAPO-5 were extracted using integrated intensities of the 210, 002, and 102/211 reflections. The intensities were corrected for the decay of the synchrotron X-ray beam using monitor counts from an ion chamber measuring the intensity of the incoming beam. Integrated intensities for the three reflections were extracted using an automatic profile fitting procedure. The crystallization curves were obtained by normalizing the sums of the integrated intensities to 1 for complete crystallization. In the case of MnAPO the crystallization was not complete for the experiment at 135 °C. Therefore, the normalization factor was set by choosing the best fit to eq 2.

Results

The preliminary crystallization experiments made at 180 °C in Teflon-lined pressure vessels gave for all four gels investigated crystalline reaction products of the [AFI] structure type. The same was observed in the *in situ* experiments, where two heating modes were used: (i) heating of the gels from 25 to 200 °C in 90 min at a constant heating rate (temperature ramp) and (ii) heating of the gels in 2 min from 25 °C to a temperature between 125 and 173 °C and keeping this temperature for 30, 60, or 120 min (isothermal). The first heating mode was applied to get an overall view of the products formed in the crystallization of the gels. The latter heating mode was used to obtain isothermal data for kinetic investigations.

Temperature Ramp. None of the four gels investigated showed formation of crystalline precursor phases before the formation of the crystalline reaction products of [AFI] type structure. Figure 2 displays the powder patterns obtained with the MnAPO-gel when heating from 25 to 200 °C in 90 min. The crystallization of the gel starts at approximately 150 °C.

Isothermal Experiments: Analysis of Crystallization Kinetics. In all the isothermal experiments, the sample was heated quickly (2 min) to the desired temperature and kept at that temperature for the duration of the data collection. Figure 3 displays the powder patterns of the MnAPO-gel at 144 °C. The Bragg reflections appear after 6−8 min at 144 °C. Figure 4 displays the powder patterns for the same gel when heated to

(27) R. J. Meyer, *Gmelins Handbuch der Anorganischen Chemie*; Verlag Chemie GmbH: Weinheim, 1970; 8. Auflage, Silber, Teil A2, p 217.
(28) Norby, P. *J. Appl. Crystallogr.* **1997**, *30*, 21.
(29) Christensen, A. N.; Norby, P.; Hanson, J. C.; Shimada, S. *J. Appl. Crystallogr.* **1996**, *29*, 265.
(30) Norby, P. *J. Am. Chem. Soc.* **1997**, *119*, 5215.

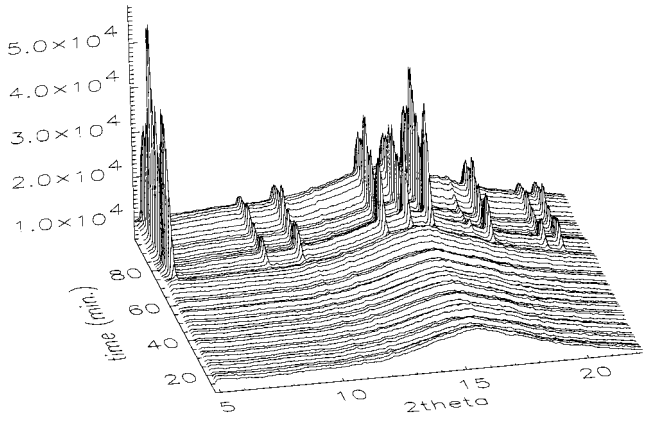

Figure 2. Stack of powder patterns obtained with the MnAPO-gel when heated from 25 to 200 °C. The reaction product is MnAPO-5, [AFI].

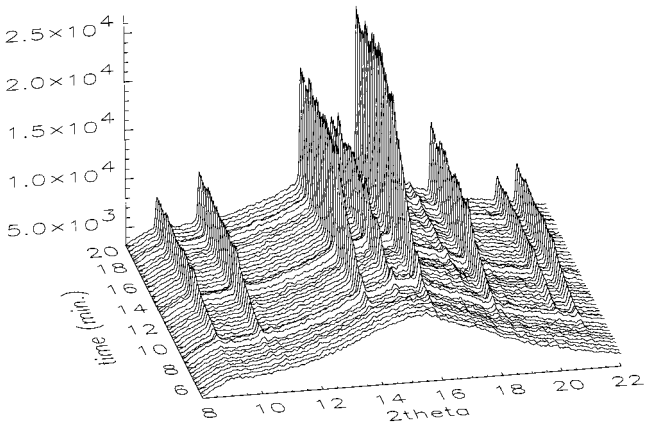

Figure 3. Stack of powder patterns obtained with the MnAPO-gel when kept at 144 °C for 30 min. The reaction product is MnAPO-5, [AFI]. The reflections used for extraction of the crystallization curve were 210, 002, and 102/211 at ca. 14, 15, and 16° in 2θ, respectively.

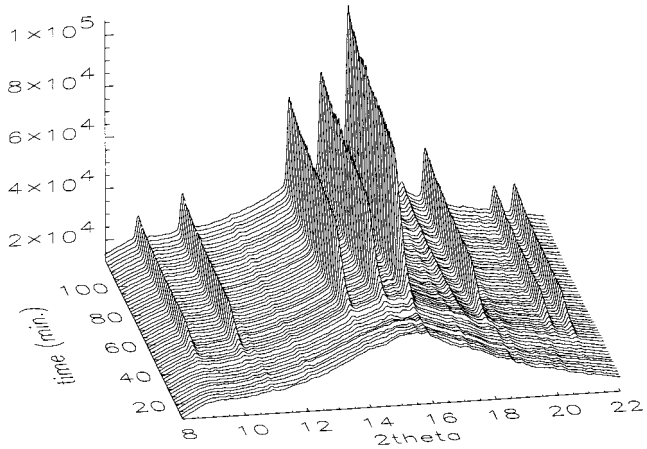

Figure 4. Stack of powder patterns obtained with the MnAPO-gel when kept at 125 °C for 120 min. The reaction product is MnAPO-5, [AFI].

125 °C, and here the Bragg reflections appear after approximately 35 min at 125 °C.

The crystallization curves for the isothermal *in situ* synthesis of Me^{2+}-substituted aluminophosphates from nonaqueous media were analyzed in order to extract kinetics information. Figure 5a−c shows the crystallization curves for MnAPO-5, MnAPO-5(HF), and CoAPO-5 at five temperatures between 125 and 173 °C. All the crystallization curves obtained displayed a sigmoidal shape. This is in contrast to previously obtained results on

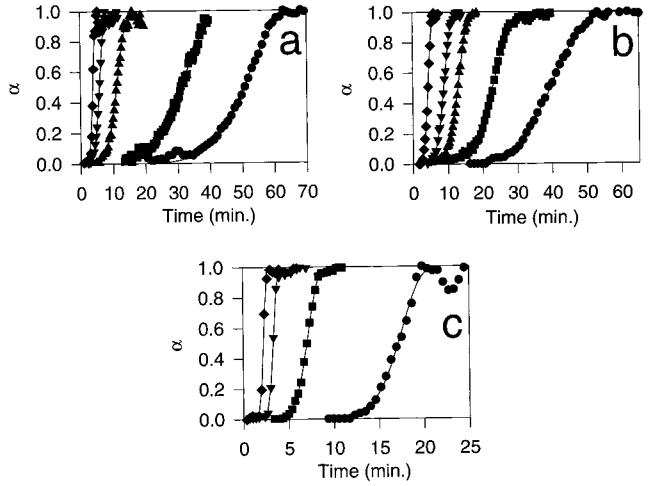

Figure 5. Crystallization curves extracted from isothermal *in situ* powder diffraction experiments at temperatures between 125 and 173 °C. Solid curves are the fits to the Avrami expression, eq 2: (a) MnAPO-5, (b) MnAPO-5(HF), and (c) CoAPO-5. Temperatures: ●, 125 °C; ■, 135 °C; ▲, 144 °C; ▼, 154 °C; ◆, 173 °C.

crystallization of Me^{2+}-substituted microporous aluminophosphates from aqueous media, where a first-order kinetics expression best described the crystallization curves.[16]

The crystallization curves for MnAPO-5, MnAPO-5(HF), and CoAPO-5 were fitted to eq 2 using the whole crystallization range, i.e., $0 < \alpha < 1$. The value of t_0 was set to 0, except for MnAPO at 173 °C, where it was necessary to fit the crystallization curve using eq 1 with a value of $t_0 = 1$ min. The crystallization curves for MnAPO-5, MnAPO-5(HF), and CoAPO-5 were also analyzed using a power law, eq 3, using the first part of the crystallization curve ($\alpha > 0.5$). Again, all curves except MnAPO at 173 °C were fitted using $t_0 = 0$. In Table 2, the Avrami parameters, k and n, are listed together with the q values obtained using eq 3. The q values are correlated to, but systematically lower than the corresponding n values, which is in agreement with earlier observations.[31] The range of determined q values is between 4 and 10.

Observed and calculated crystallization curves are given in Figure 5a−c. The values for the rate constants and exponents (n) obtained from fitting eq 2 to the crystallization curves are listed in Table 2. The values obtained for n lie in the range 6−10. The rate constants, k, for the crystallization curves were extracted using individual n values. As stated earlier, the modified Avrami equation (eq 2) results in consistent k values independent of n.

To verify the values of n obtained by the Avrami fit, $\ln(-\ln(1-\alpha))$ was plotted against $\ln(t)$ for all experiments. According to eq 2, this should give a straight line with slope n. Figure 6a shows $\ln(-\ln(1-\alpha))$ plotted against $\ln(t)$ for the crystallization of MnAPO-5(HF) for values of α between 0.1 and 0.95. The values of n obtained by linear fits to the data are given in Figure 6a and compare very well with those obtained by direct fitting with the modified Avrami equation, Table 2.

It is difficult to compare crystallization curves at different temperatures when they are plotted as a function of time, as in Figure 5. However, crystallization curves plotted as a function of kt become independent of temperature for a constant value of n, according to eq 2. Figure 6b shows the observed crystallization curves for MnAPO-5(HF) plotted on a normalized time scale using the k values obtained from the Avrami fit. As

(31) Gualtieri, A.; Norby, P.; Artioli, G.; Hanson, J. C. *Phys. Chem. Min.* **1997**, *24*, 191.

Table 2. Kinetics Data for Crystallization of Mn- and Co-Substituted Aluminophosphates from Nonaqueous Media[a,b]

	MnAPO-5				MnAPO-5(HF)				CoAPO-5			
T (°C)	k (min^{-1})	n	q	$t_{0.63}$ (min)	k (min^{-1})	n	q	$t_{0.63}$ (min)	k (min^{-1})	n	q	$t_{0.63}$ (min)
125	0.0188(1)	7.1(2)	5.1(2)	53.4	0.0238(5)	5.8(1)	5.2(1)	42.0	0.0561(3)	9.8(5)	7.8(5)	18.0
135	0.0306(1)	5.4(1)	3.9(1)	33.5	0.0413(1)	6.2(2)	4.9(2)	24.0	0.136(4)	8.1(2)	7.2(2)	7.3
144	0.0837(5)	5.6(2)	4.9(1)	11.9	0.0736(2)	6.9(1)	5.7(1)	13.5				
154	0.161(1)	5.8(3)	4.4(1)	6.3	0.107(2)	6.1(1)	5.2(2)	9.4	0.292(1)	10.5(7)	9.6(6)	3.4
173	0.340(3)[c]	6.5(5)[c]	5.7(3)[c]	4.0	0.218(1)	5.7(2)	4.6(2)	4.6	0.434(3)	10.0(1)	8.4(5)	2.3

[a] The crystallization cruves were fitted using the modified Avrami equation: $\alpha(t) = 1 - \exp(-(kt)^n)$. q values were found by fitting the first part of the crystallization curve ($\alpha < 0.5$) to the expression $\alpha = at^q$. The values for $t_{0.63}$ were determined as the time when $\alpha = 0.63$. Apparent activation energies determined from Arrhenius plots of ln(k) vs 1000/T were as follows: MnAPO-5, 94(9) kJ/mol; MnAPO-5(HF), 68(4) kJ/mol; CoAPO-5, 61(11) kJ/mol. [b] The parameters found for aqueous crystallization of $AlPO_4$-5 at 173 °C were $k = 0.053(1)$ min^{-1}, $n = 1.8(6)$. [c] The parameters for MnAPO-5 at 173 °C were fitted using $t_0 = 1$ min.

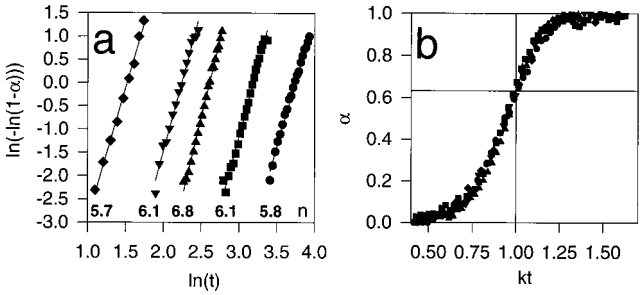

Figure 6. (a) Plot of ln(−ln(1 − α)) vs ln(t) for crystallization of MnAPO-5(HF) between 125 and 173 °C. Solid lines are linear fits to each curve, and the value of n is the slope of the lines according to eq 2. (b) The crystallization curves for MnAPO-5(HF) plotted on a normalized time scale, kt, where k is the individual rate constant obtained from fitting the curves to eq 2. The point where $kt = 1$ and $\alpha(kt) = 1 - e^{-1}$ is indicated. Temperatures: ●, 125 °C; ■, 135 °C; ▲, 144 °C; ▼, 154 °C; ◆, 173 °C.

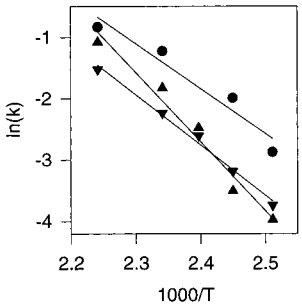

Figure 7. Arrhenius plots, ln(k) vs 1000/T, for isothermal crystallization of MnAPO-5 (▲), MnAPO-5(HF) (▼), and CoAPO-5 (●). From the slopes of the linear regression lines, apparent activation energies were derived (Table 2).

seen from Figure 6b, the curves $\alpha(kt)$ are almost coinciding, in good agreement with the small variation of n found from the refinement. In this type of plot the sigmoidal shapes of all the crystallization curves are clearly seen. According to eq 2, all the curves plotted on a normalized time scale should have the value $\alpha = 0.63$ for $kt = 1$. This point is marked in Figure 6b by intersecting lines and is seen to agree well with the observed curves.

The obtained rate constants were used to find apparent activation energies for the crystallization process using the Arrhenius expression, eq 4. In Figure 7, ln(k) is plotted against 1000/T, and the obtained linear fits are shown as solid lines. Apparent activation energies for crystallization of MnAPO-5, MnAPO-5(HF), and CoAPO-5 were found to be 94, 68, and 61 kJ/mol, respectively.

Discussion

The crystallization curves obtained from time resolved *in situ* powder diffraction studies of crystallization of Me^{2+}-substituted microporous aluminophosphates with [AFI]-type structures, all clearly showed a sigmoidal shape (Figure 5). The curves could be very well described using a modified Avrami expression, eq 2.

There is a striking difference between the values of n obtained from aqueous and nonaqueous systems, as reflected in the shape of the crystallization curves. Crystallization of MnAPO-5 showed a first-order behavior,[16] i.e., $n = 1$. The crystallization curves for CoAPO-5 showed some sigmoidal shape.[32] By fitting the original data using the Avrami expression, using a least-squares method, n refined to 1.8. Crystallization curves for CoAPO-5 reported in an early *in situ* powder diffraction study[33] also showed first-order behavior. In contrast to this, values of n obtained from nonaqueous synthesis of MnAPO-5 in this study gave values of n between 5 and 7. For CoAPO-5 the values were even higher, between 8 and 10 (Table 2), which is among the highest n values reported for zeolite crystallization curves.

As seen from Figure 1, a high value of n means that the initial crystallization rate is small but that it increases rapidly at a later stage.

It is often found that crystallization from nonaqueous media results in larger crystals than obtained from aqueous synthesis. This seems to be in contrast to the observation of an explosive increase in crystallization rates, which is often explained by autocatalytic nucleation.[25] However, growth of larger crystals may occur on a longer time scale by dissolution of the crystals initially formed, and subsequent recrystallization. There may very well be an effect of the added mineralizer in this process, which can explain the formation of larger crystals after longer reaction times. This is, however, beyond the scope of the present investigation.

The crystallization rates of MnAPO-5 and CoAPO-5 from nonaqueous solution obtained from the time resolved *in situ* experiments performed here are not directly comparable to reported crystallization rates from aqueous media, as reported earlier.[16] However, although the chemical composition differs, some qualitative comparisons of crystallization behavior may be made. The crystallization of MnAPO-5 reported in ref 16 is much slower than found in this study. In an *in situ* study[32] of crystallization of CoAPO-5, crystallization times were found to be comparable with the ones obtained for nonaqueous synthesis. One experiment was performed in the present investigation, crystallizing $AlPO_4$-5 from aqueous solution at 173 °C. The obtained rate constants and n values are reported in Table 2. In this experiment, crystallization was much slower than for the nonaqueous synthesis. It must be concluded that

(32) Norby, P.; Hanson, J. C. *Catal. Today* **1998**, *39*, 301.
(33) Norby, P.; Nørlund Christensen, A.; Hanson, J. C. In *Studies in Surface Science and Catalysis*; Weitkamp, H. G., Karge, H., Pfeifer, Hölderich, Eds.; Elsevier: Amsterdam, 1994; Vol. 84, p 179.

very small changes in, for instance, pH and chemical composition may have a significant influence on the crystallization rate.

Comparative experiments were performed in which MnAPO-5 was crystallized at several different temperatures, with and without HF as a mineralizing agent. In Figure 5 the crystallization curves are shown, and in Table 2 the rate constants and *n* values are listed. No dramatic differences between the experiment with and without added HF are seen. The *n* values determined from the two series of experiments were not significantly different, ranging between 5 and 7, and the crystallization rates were comparable. From an Arrhenius plot, Figure 7, the apparent activation energies for crystallization of MnAPO-5 and MnAPO-5(HF) were determined as 94 and 68 kJ/mol, respectively. The experiment indicates that addition of HF to the reaction mixture reduces the apparent activation energy. It must be emphasized that this result is based on only one experiment and that additional experiments are necessary in order to confirm the result. The apparent activation energies determined are comparable with values found from crystallization of MnAPO-5 from aqueous media.[16] Using first-order kinetics analysis, the apparent activation energy for crystallization was determined to be 81 kJ/mol.

When comparing the results from the *in situ* crystallization of Mn and Co substituted aluminophosphates, it is clear that crystallization is significantly faster for CoAPO-5 than for MnAPO-5. The difference in crystallization rates is also seen in Table 2 from the time it takes to reach 63% completion, $t_{0.63}$. Also, the derived apparent activation energies, Figure 7, are different: 61 kJ/mol for CoAPO-5 vs 94 kJ/mol for Mn-APO-5. The apparent activation energy determined for CoAPO-5 is comparable with the one found for MnAPO-5(HF), where HF was added as a mineralizing agent. The crystallization in nonaqueous media progresses faster for CoAPO-5 than for MnAPO-5.

Conclusions

Time-resolved *in situ* X-ray synchrotron powder diffraction is a powerful tool for studying synthesis and chemical reactions involving crystalline materials. The crystallization of MAPO-5, M = (Co, Mn), was followed *in situ* at different temperatures, and the effect of adding HF as a mineralizing agent was investigated.

Crystallization curves for all experiments could be described well using an Avrami-type kinetic expression: $\alpha(t) = \exp(-(kt)^n)$.

The values obtained for *n* were found to be generally higher for the ethylene glycol system than those reported for crystallization in pure aqueous systems. This indicates a change in nucleation mechanism when the synthesis is performed in ethylene glycol.

The apparent activation energy for crystallization of MnAPO-5 was found to be significantly higher than for CoAPO-5. At the same time, crystallization of CoAPO-5 was faster than for MnAPO-5, while the values of *n* obtained for CoAPO-5 were significantly higher than for MnAPO-5. Thus, the nature of the transition metal cation seems to have a significant influence on the crystallization rate as well as the crystallization mechanism.

A decrease in apparent activation energy for crystallization of MnAPO-5 was found when adding HF to the reaction mixture, while the crystallization rates and the values obtained for *n* were comparable. However, further experiments are needed in order to investigate if lowering of apparent activation energies by adding HF is a general trend and to obtain details regarding the relation between activation energy and crystal growth.

It was shown that for crystallization curves with Avrami-type behavior the time for half-completion, $t_{0.5}$, is not the best choice for evaluation of reaction kinetics and energetics. It is in general advantageous to use the time for 63% completion, $t_{0.63}$. At this point the rate constant can be determined as $k = 1/t_{0.63}$, independent of the value of *n*.

Acknowledgment. The Danish Natural Science Research Council has supported this investigation with grants. The synchrotron X-ray measurements were carried out at Brookhaven National Laboratory, supported under contract DE-AC02-76CH00016 with the US Department of Energy by its Division of Chemical Sciences Office of Basic and Energy Science. Mrs. M. A. Chevallier, Mrs. C. Secher, Mr. A. Lindahl, and Mr. N. J. Hansen are acknowledged for valuable assistance.

IC980749Z